The Journal of Microbiology (2012) Vol. 50, No. 5, pp. 777–784
DOI 10.1007/s12275-012-2187-1


# Identification and Characterization of an Autolysin Gene, *atlA*, from *Streptococcus criceti*

**Haruki Tamura*, Arisa Yamada, and Hirohisa Kato**

*Division of Bioregulatory Pharmacology, Department of Pharmacology, Iwate Medical University, 2-1-1 Nishitokuta, Yahaba-cho 028-3694, Japan*

(Received April 10, 2012 / Accepted June 29, 2012)

**AtlA of *Streptococcus mutans* is a major autolysin and belongs to glycoside hydrolase family 25 with cellosyl of *Streptomyces coelicolor*. The autolysin gene (*atlA*) encoding AtlA was identified from *S. criceti*. AtlA of *S. criceti* comprises the signal sequence in the N-terminus, the putative cell-wall-binding domain in the middle, and the catalytic domain in the C-terminus. Homology modeling analysis of the catalytic domain of AtlA showed the resemblance of the spatial arrangement of five amino acids around the predicted catalytic cavity to that of cellosyl. Recombinant AtlA and its four point mutants, D655A, D747A, W831A, and D849A, were evaluated on zymogram of *S. criceti* cells. Lytic activity was destroyed in the mutants D655A and D747A and diminished in the mutants W831A and D849A. These results suggest that Asp655 and Asp747 residues are critical for lytic activity and Trp831 and Asp849 residues are also associated with enzymatic activity.**

***Keywords***: degenerate PCR, homology modeling, site-directed mutagenesis, zymogram assay

## Introduction

*Streptococcus mutans* comprises a major autolysin AtlA, in which two isoforms, 107 and 79 kDa, are preserved (Shibata *et al.*, 2005). This molecule is involved in cell separation, biofilm formation, and genetic competence (Shibata *et al.*, 2005; Ahn and Burne, 2006), and is considered as a potential target for the control of biofilm formation (Shibata *et al.*, 2005). AtlA, also referred to Aml, is an *N*-acetylmuramidase, which selectively lyses two cariogenic organisms in humans, *S. mutans* and *Streptococcus sobrinus* (Hamada and Slade, 1980; Yoshimura *et al.*, 2006), and its lytic activity is enhanced in the presence of calcium ions (Yoshimura *et al.*, 2006). To date, AtlG of *S. sobrinus* and AtlH of *S. downei* have been identified in mutans streptococci (Tamura *et al.*, 2009; Yamada *et al.*, 2009). These autolysins belong to glycoside hydrolase family 25 (GH25) in the CAZy database (Cantarel *et al.*, 2009) and are modular enzymes consisting of a signal sequence in the N-terminus (24–30 amino acid residues), a putative cell-wall-binding domain (631–751 amino acid residues) in the middle, and a catalytic domain (202–204 amino acid residues) in the C-terminus (Shibata *et al.*, 2005; Tamura *et al.*, 2009; Yamada *et al.*, 2009). In the putative cell-wall-binding domain, 15-residue repeats are copied from four to five times (Yoshimura *et al.*, 2006; Tamura *et al.*, 2009; Yamada *et al.*, 2009). In the catalytic domain of AtlA, Asp869 is a critical residue for lytic activity (Yoshimura *et al.*, 2006).

Until now, four members of GH25, cellosyl of *Streptomyces coelicolor* (Rau *et al.*, 2001), Cpl-1 of pneumococcal phage Cp-1 (Hermoso *et al.*, 2003), LytC of *Streptococcus pneumoniae* (Pérez-Dorado *et al.*, 2010), and *Ba*GH25c of *Bacillus anthracis* (Martinez-Fleites *et al.*, 2009) have been structurally characterized by their catalytic regions as an irregular $(\beta/\alpha)_5\beta_3$ barrel fold. Alternatively, there is a discrete approach towards the elucidation of protein structures. Homology modeling, also called comparative protein structure modeling, is a computational method for building three-dimensional models of proteins from the identified structure of the template protein on the basis of amino acid sequence alignment (Le *et al.*, 2004; Chávez-Gutiérrez *et al.*, 2006; Bordoli *et al.*, 2009).

*Streptococcus criceti*, a member of mutans streptococci, is a cariogenic agent in animals and rarely isolated from humans (Loesche, 1986). No information on autolysins has previously been available for *S. criceti*. In the present study, we first identified the autolysin gene (*atlA*) of *S. criceti*, and characterized the gene products by homology modeling and site-directed mutagenesis.

## Materials and Methods

### Bacterial strains and culture conditions

*S. criceti* strains E49 and ATCC 19642$^T$ were grown anaerobically at 37°C in brain-heart infusion broth (Difco Laboratories, USA). *Escherichia coli* strains JM109 and BL21(DE3) (EMD Chemicals, USA), used for cloning and expressing proteins, respectively, were grown in Luria-Bertani medium (Difco Laboratories) at 37°C. If necessary, 50 μg/ml ampicillin was used.

### DNA manipulation

Purification of chromosomal DNA of bacteria and DNA sequencing were carried out as described previously (Yamada *et al.*, 2009). Plasmid DNA purification was performed using

*For correspondence. E-mail: htamura@iwate-med.ac.jp; Tel.: +81-19-651-5111

**Table 1.** Oligonucleotide primers

| Designation | Sequence (5′ to 3′) | Reference |
|---|---|---|
| Degenerate PCR of *atlA* gene | | |
| DP-F2 | ATGGTNCCNGTNTGGWSNGAYCARAA | This study |
| DP-R | GTRTAYTGCCANGCNGCNGCRTT | Tamura *et al.* (2009) |
| Gene-walking of *atlA* gene | | |
| GW126 | AGCTGCTAAGCCTACCAAGCCACCTGTAAT | This study |
| GW127 | CGAGGTGGTAGTTTCTCAACAGGCCAAGT | This study |
| Sequencing of *atlA* gene in *S. criceti* ATCC 19642$^T$ | | |
| HS6F | GACATTAAGGCCCTGCGAAAGA | This study |
| HS6R | GCAATATCAACCTTGAGTGGTTTTA | This study |
| Construction of His-tagged AtlA | | |
| AtlA-FN | AATATACATATGGATGAAACCAGTGATGTTCCAG | This study |
| AtlA-RX | AAAATGCTCGAGACTCAAACGACCTGTATAGTCAATACT | This study |
| Construction of His-tagged D655A, an AtlA derivative | | |
| D655A-F | TTTATCG**C**CGTCAGCAGCTA | This study |
| D655A-R | CTGCTGACG**G**CGATAAAGTA | This study |
| Construction of His-tagged D747A, an AtlA derivative | | |
| D747A-F | ATGGTTGATG**C**TATTGAAGCAA | This study |
| D747A-R | TTGCTTCAATA**G**CATCAACCAT | This study |
| Construction of His-tagged W831A, an AtlA derivative | | |
| W831A-F | CGGCAGCT**GC**GCAATATA | This study |
| W831A-R | GTATATTGC**GC**AGCTGCCGCATT | This study |
| Construction of His-tagged D849A, an AtlA derivative | | |
| D849A-RX | TTTTTGCTCGAGACTCAAACGACCTGTATAG**G**CAATACTT | This study |

Degenerate primers DP-F2 and DP-R were designed from the deduced amino acid sequence of *S. mutans* AtlA (Shibata *et al.*, 2005): MVPVWSDQN (residues 300–308) and NAAAWQY (residues 949–955), respectively. Restriction sites of *Nde*I and *Xho*I are underlined. Positions mutated for AtlA derivatives are shown in bold.

NucleoSpin Plasmid (Macherey-Nagel GmbH, Germany). *E. coli* transformation was carried out by the calcium chloride procedure (Hanahan, 1983).

### DNA sequence analysis

The nucleotide sequences were determined with a BigDye Terminator v3.1 Cycle Sequencing Kit (Applied Biosystems, USA) as described previously (Yamada *et al.*, 2009). The software GENETYX Ver.11 (Genetyx, Japan) was used for sequence analysis. Multiple alignments of the deduced amino acid sequences were generated using CLUSTAL X 2.1 (Larkin *et al.*, 2007) and phylogenetic trees obtained with the neighbor-joining method were depicted by TreeView 1.66 (Page, 1996).

### PCR experiments

To determine a part of the *atlA* gene, degenerate PCR was performed with primers DP-F2 and DP-R (Tamura *et al.*, 2009) (Table 1). The amplified 1,676-bp fragment designated DP was cloned into pGEM-T vector (Promega, USA) and sequenced. The adjacent region of DP was determined by the gene-walking method with the first internal primers GW126 and GW127, as described previously (Tamura *et al.*, 2007). To determine the nucleotide sequence of the *atlA* gene in *S. criceti* ATCC 19642$^T$, PCR was carried out with primers HS6F and HS6R (Table 1).

### Cloning, expression, and purification of histidine-tagged proteins

To express AtlA with a C-terminal six histidine tag, PCR fragment amplified with primers AtlA-FN and AtlA-RX was digested with *Nde*I and *Xho*I and inserted into the corresponding sites of pET-21a(+) (EMD Chemicals), resulting in plasmid pET21aatlA carrying AtlA (residues 32–855). To construct plasmid pET21aD655A expressing a D655A point mutant, PCR-based mutagenesis (Ho *et al.*, 1989) was performed with three pairs of primers: AtlA-FN/D655A-R, D655A-F/AtlA-RX, and AtlA-FN/AtlA-RX; pET21aD747A and pET21aW831A were also constructed. Plasmid pET21a-D849A for mutant D849A was constructed using a PCR fragment with primers AtlA-FN and D849A-RX. Nucleotide sequences of the constructs were confirmed by sequencing on both strands. Protein expression system for *E. coli* was used and purification of recombinant AtlA and its derivatives using Ni Sepharose 6 Fast Flow (GE Healthcare UK Ltd., UK) was performed as described previously (Tamura *et al.*, 2009). Protein analysis by sodium dodecyl sulfate-polyacrylamide gel electrophoresis (SDS-PAGE) was carried out as described (Tamura *et al.*, 2009).

### Zymogram assay

Extraction of autolytic proteins of cells in 4% (w/v) SDS and preparation of hydrofluoric acid (HF)-treated *S. criceti* E49 cells were performed as described previously (Tamura *et al.*, 2009). $NaN_3$-treated *S. criceti* E49 cells were obtained as follows. Overnight cultured cells were suspended in 1% (w/v) sodium azide and washed three times in distilled water. Cells were resuspended in SDS-7.5% acrylamide solution to an $OD_{600}$ of 1.0 for SDS-PAGE. The protein samples were separated on gels incorporating HF- and $NaN_3$-treated cells and renatured for 5 h at 37°C with 1 mM $CaCl_2$ as described

previously (Tamura *et al.*, 2009). The gels were photographed, and translucent bands were evaluated by ImageJ (Abràmoff *et al.*, 2004). The results shown in the figures are representative, and all the observations were confirmed in three separate experiments.

### Homology modeling

Comparative modeling of the catalytic domain of AtlA was performed using the 3D-JIGSAW 2.0 program (Bates *et al.*, 2001). Generated models were validated using PROCHECK (Laskowski *et al.*, 1993) and VERIFY 3D (Lüthy *et al.*, 1992). Realignment, modeling and validation were repeated until an appropriate model was obtained. Models were analyzed by Swiss-PdbViewer 4.0.1 (Guex and Peitsch, 1997) and depicted by UCSF Chimera 1.4.1 (Pettersen *et al.*, 2004).

### Nucleotide sequence accession numbers

The 9,358-bp (*S. criceti* E49) and 3,453-bp (*S. criceti* ATCC 19642$^T$) nucleotide sequences determined in this study have been assigned under GenBank accession numbers AB381882 and AB477107, respectively.

## Results

### Sequence analysis

Nucleotide sequence analysis revealed that nine open reading frames (ORFs) in the 9,358-bp region of *S. criceti* E49 and ORF1 and ORF9 were incomplete and the others were complete ORFs. ORF6 was designated *atlA* (Fig. 1A). The amino acid sequences deduced from these ORFs showed homology to those of the gene products found in *S. mutans*, *S. downei*, and *S. sobrinus*. Comparing to the predicted gene products of *S. mutans* UA159, a completely sequenced strain (Ajdić *et al.*, 2002), the amino acid sequences deduced from first, second, third, and fifth ORFs showed 57.6, 78.0, 46.8, and 91.1% identity to the gene products encoded by SMU.1417c, SMU.1415c, SMU.1414c, and SMU.1394, respectively, which are situated at discrete gene loci from *atlA* (SMU.689). The deduced amino acid sequence of ORF4 showed no homology to amino acid sequences deduced from genes in *S. mutans* but exhibited 82.6% identity to the nucleoside diphosphate kinase of *S. downei* F0415 (GenBank accession no. EFQ56561). The amino acid sequences deduced from ORF7, ORF8, and ORF9 in the downstream region of the *atlA* showed 62.2, 62.3, and 88.4% identity to those encoded by SMU.692 (*thmA*), SMU.695, and SMU.696, respectively, which are located in the region downstream of *atlA* (SMU.689). However, genes homologous to SMU.688, SMU.690, and SMU.691 were not observed in the sequenced region in *S. criceti* E49, as they are not in the *atlG* region of *S. sobrinus* 6715DP (Yamada *et al.*, 2009). In comparison with the *atlG* region of *S. sobrinus* 6715DP, the amino acid sequences deduced from fifth, seventh, eighth, and ninth ORFs demonstrated 95.2, 87.4, 69.7, and 97.7% identity to the gene products encoded by ORF1, ORF3, ORF4, and ORF5, respectively, which are flanked with ORF2 (*atlG*)

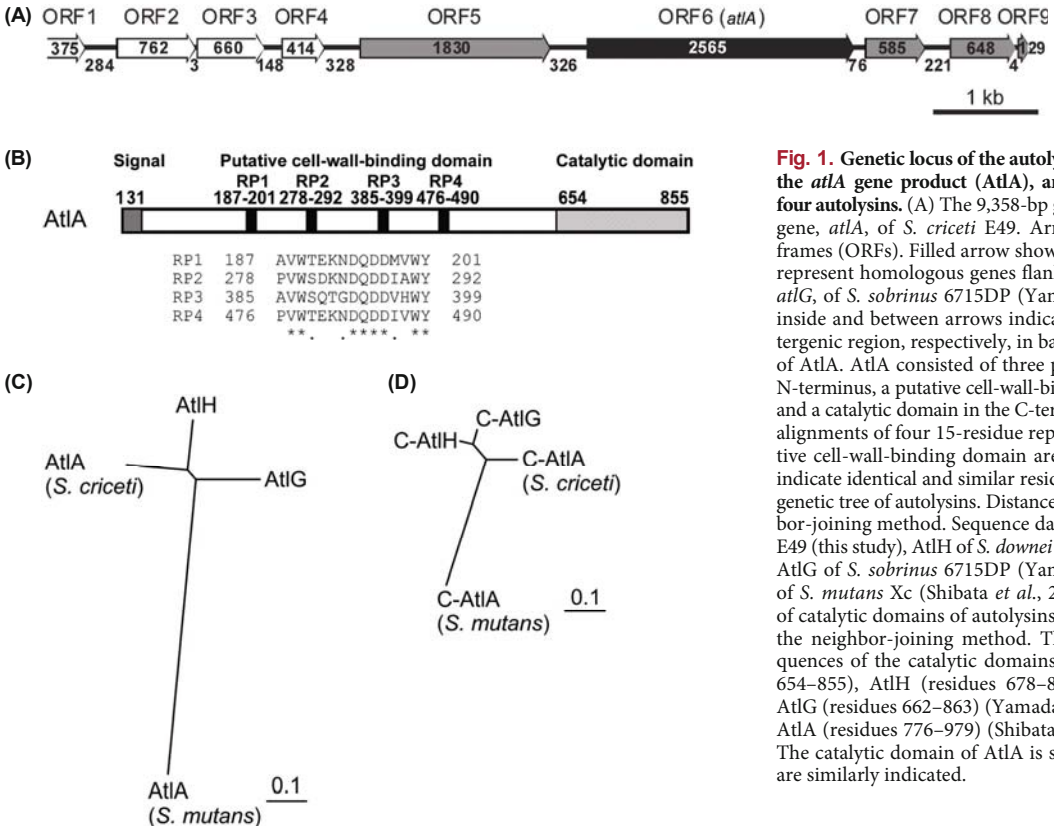


**Fig. 1. Genetic locus of the autolysin gene (*atlA*), structure of the *atlA* gene product (AtlA), and phylogenetic analyses of four autolysins.** (A) The 9,358-bp genetic locus of the autolysin gene, *atlA*, of *S. criceti* E49. Arrows indicate open reading frames (ORFs). Filled arrow shows *atlA* gene and gray arrows represent homologous genes flanked with the autolysin gene, *atlG*, of *S. sobrinus* 6715DP (Yamada *et al.*, 2009). Numbers inside and between arrows indicate the size of ORFs and intergenic region, respectively, in base pairs. (B) Structural traits of AtlA. AtlA consisted of three parts: a signal peptide in the N-terminus, a putative cell-wall-binding domain in the middle, and a catalytic domain in the C-terminus. Amino acid sequence alignments of four 15-residue repeats (RP1–RP4) in the putative cell-wall-binding domain are shown. Asterisks and dots indicate identical and similar residues, respectively. (C) Phylogenetic tree of autolysins. Distance was calculated by the neighbor-joining method. Sequence data are from AtlA of *S. criceti* E49 (this study), AtlH of *S. downei* MFe28 (Tamura *et al.*, 2009), AtlG of *S. sobrinus* 6715DP (Yamada *et al.*, 2009), and AtlA of *S. mutans* Xc (Shibata *et al.*, 2005). (D) Phylogenetic tree of catalytic domains of autolysins. Distance was calculated by the neighbor-joining method. The deduced amino acid sequences of the catalytic domains of *S. criceti* AtlA (residues 654–855), AtlH (residues 678–879) (Tamura *et al.*, 2009), AtlG (residues 662–863) (Yamada *et al.*, 2009), and *S. mutans* AtlA (residues 776–979) (Shibata *et al.*, 2005) were analyzed. The catalytic domain of AtlA is shown as C-AtlA and others are similarly indicated.

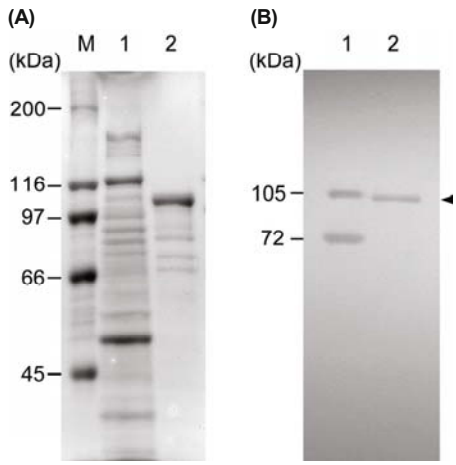


**Fig. 2. Coomassie brilliant blue-stained SDS-polyacrylamide gel and zymogram of 4% SDS extracts of *S. criceti* E49 and recombinant AtlA.** (A) Protein profiles on SDS-polyacrylamide gel stained with Coomassie brilliant blue. (B) Zymogram of HF-treated *S. criceti* E49 cells. Arrowhead indicates the position of 103 kDa. Lanes: 1, 4% SDS extracts of *S. criceti* E49; 2, recombinant AtlA; M, molecular marker.

encoding a major autolysin AtlG of *S. sobrinus* 6715DP (Yamada *et al.*, 2009), suggesting the similarity of the adjacent region of *atlA* to that of *atlG*.

The 3,453-bp nucleotide sequence of the *atlA* gene and flanking region of *S. criceti* ATCC 19642$^T$ was identical to those of the *atlA* gene of *S. criceti* E49. A putative promoter sequence, TTGATA-$N_{19}$-TAACTT, was found 32 bp upstream from the start codon for *atlA*. The *atlA* gene was preceded by a putative ribosome binding site (AGGA) located 10 bp in front of the initiation codon. The predicted translational product of the *atlA*, AtlA, was a protein of 855 amino acids with a molecular weight of 93,151.53 and pI of 5.04. A 31-amino-acid signal sequence was predicted in the N-terminus (Fig. 1B). Four 15-residue repeats RP1 to 4 were found in the putative cell-wall-binding domain as well as four repeats in AtlH of *S. downei* MFe28 (Tamura *et al.*, 2009) and AtlG (Yamada *et al.*, 2009) and were separated by 76-, 92-, and 76-amino-acid residues, respectively. A catalytic domain homologous to those of GH25 in the CAZy database (Cantarel *et al.*, 2009) was predicted in the C-terminus. At the amino acid sequence level, AtlA showed 70.1, 63.4, and 40.9% identity to AtlH (Tamura *et al.*, 2009), AtlG (Yamada *et al.*, 2009), and AtlA of *S. mutans* Xc (Shibata *et al.*, 2005), respectively. Phylogenetic analyses of the whole and the catalytic domains of the four autolysins showed the resemblance between AtlA (*S. criceti*) and AtlH (Fig. 1C) and the resemblance between C-AtlG (catalytic domain of AtlG) and C-AtlH (catalytic domain of AtlH) (Fig. 1D), respectively, suggesting that, overall, AtlA (*S. criceti*) resembled AtlH in the four autolysins.

## Zymographic analysis of SDS extracts and AtlA

As SDS extracts of cells comprise autolysins (Shibata *et al.*, 2005; Tamura *et al.*, 2009), SDS extracts of *S. criceti* E49 were

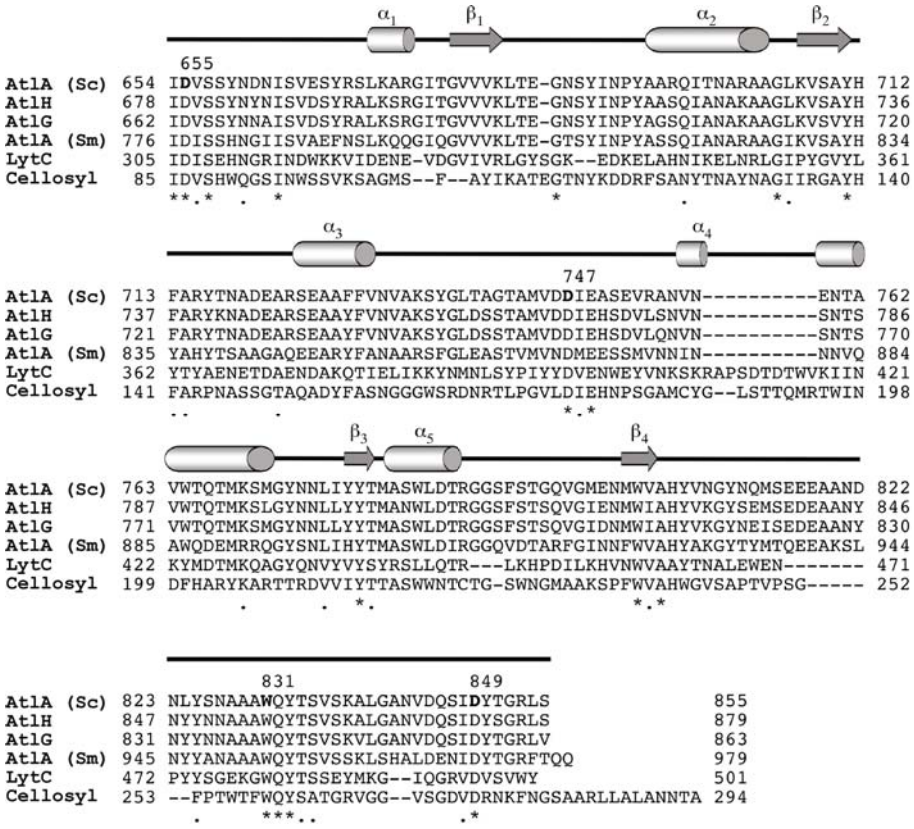


**Fig. 3. Comparison of the amino acid sequence of catalytic domains of GH25 members.** The positions of site-directed mutagenesis for AtlA are shown in bold. Estimated secondary structure of the catalytic domain of AtlA is shown above the sequence alignments. α-Helix and β-strands are depicted as cylinders and arrows, respectively. Sequences shown here are from AtlA (this study), AtlH (Tamura *et al.*, 2009), AtlG (Yamada *et al.*, 2009), AtlA (Shibata *et al.*, 2005), LytC of *Streptococcus pneumoniae* (GenBank accession no. AJ009639), and cellosyl of *Streptomyces coelicolor* (Rau *et al.*, 2001). AtlA (Sc), AtlA of *S. criceti*; AtlA (Sm), AtlA of *S. mutans*.

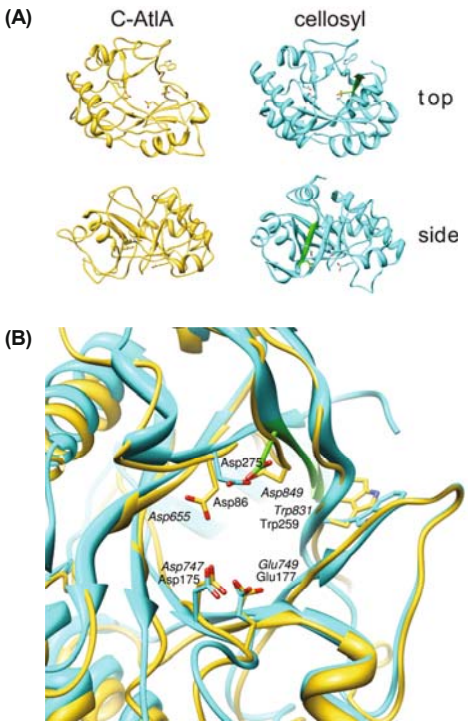


**Fig. 4. The three-dimensional structural models of the catalytic domain of AtlA (C-AtlA) and cellosyl.** (A) Comparison of a computational model of the catalytic domain of AtlA, C-AtlA, with the template model of cellosyl. Three-dimensional structure of cellosyl was obtained from the Structural Bioinformatics Protein Data Bank under PDB 1JFX (Rau *et al.*, 2001). C-AtlA and cellosyl are in gold and cyan, respectively. The anti-parallel β-strand of cellosyl ($\beta_8$) is in green. (B) Superposition of the catalytic cavities of C-AtlA (gold) and cellosyl (cyan). Putative catalytic residues of AtlA and cellosyl are shown as ball-and-stick figures labeled with and without italics, respectively.

analyzed with recombinant AtlA of *S. criceti* by SDS-PAGE and zymography (Figs. 2A and 2B). Two bands, 105- and 72-kDa, were detected in the SDS extracts of *S. criceti* cells (Fig. 2B, lane 1). In *S. mutans*, 107- and 79-kDa bands observed in the SDS extracts originated from AtlA (Shibata *et al.*, 2005), suggesting that two bands of the SDS extracts might be derived from AtlA of *S. criceti*. A 103-kDa band was observed in recombinant AtlA (Fig. 2B, lane 2). In the zymogram, the band intensity of the recombinant AtlA was weaker than those of the 105- and 72-kDa bands of the SDS extracts.

### A computational model of catalytic domain of AtlA

Three-dimensional models of the catalytic domain of AtlA were computationally built using the structure of cellosyl (Rau *et al.*, 2001) (PDB code 1JFX; 28% sequence identity to the catalytic domain of AtlA) as a template and the model showed no further improvement by realignment. In contrast, construction of a computational model of the putative cell-wall-binding domain of AtlA failed because no template structure was suitable for modeling. The Ramachandran plot in the PROCHECK showed that 97.3% (180 residues) of the 185 non-glycine and non-proline residues were in the allowed region and 2.7% of the residues (5 residues) were in the disallowed region. Analysis of the template and model with VERIFY 3D showed that the Z-score of the template was 0.77 and that of the model was 0.62. These results suggest that the proposed model is acceptable.

In the generated model, the catalytic region of AtlA comprised five α-helices ($\alpha_1$–$\alpha_5$) and four β-strands ($\beta_1$–$\beta_4$) (Fig. 3). This differed from cellosyl, which contains five α-helices and eight β-strands and exhibits an irregular $(\beta/\alpha)_5\beta_3$ fold different from triose phosphate isomerase and possesses the anti-parallel orientation of strand $\beta_8$, which is characteristic of the GH25 family (Rau *et al.*, 2001). The strands corresponding to $\beta_1$, $\beta_4$, $\beta_7$, and $\beta_8$ in cellosyl were absent in the model of the catalytic domain of AtlA; however, the amino acid sequences of AtlA, Asp655, Asp747, Glu749, Trp831, and Asp849 were identical to the corresponding sequences of cellosyl, Asp86, Asp175, Glu177, Trp259, and Asp275, respectively, on strands $\beta_1$, $\beta_4$, $\beta_7$, and $\beta_8$. In cellosyl, the three residues, Asp86, Asp175, and Glu177, were considered as candidates for catalytically active residues (Rau *et al.*, 2001).

The predicted model of the catalytic domain of AtlA resembled the spatial structure of cellosyl, albeit with low sequence identity and low conservation of the secondary structure (Fig. 4A). Although the orientation of the Asp655 of AtlA was different from that of Asp86 of cellosyl, the

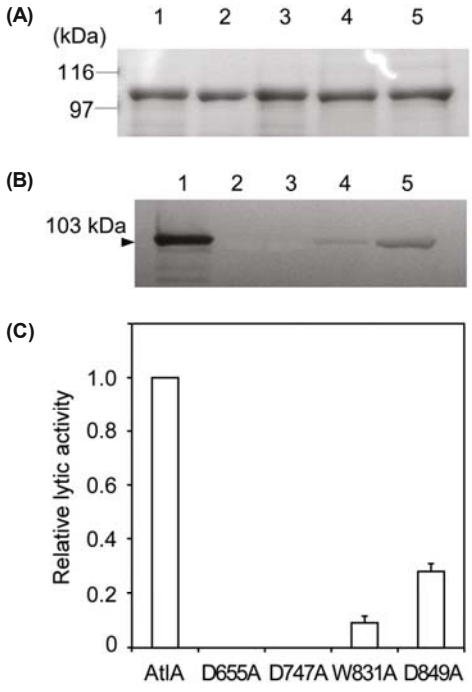


**Fig. 5. Lytic activities of recombinant AtlA and its derivatives.** (A) Coomassie brilliant blue staining of SDS-polyacrylamide gel. (B) Zymographic patterns of AtlA and four AtlA derivatives on $NaN_3$-treated *S. criceti* E49 cells. Proteins (10 μg each) were loaded. Arrowhead indicates the position of 103 kDa. Lanes: 1, AtlA; 2, D655A; 3, D747A; 4, W831A; 5, D849A. (C) Relative lytic activities of AtlA derivatives. Relative lytic activities of AtlA derivatives to wild-type AtlA were evaluated by ImageJ (Abràmoff *et al.*, 2004). The values are expressed as a ratio with wild-type AtlA. The results represent the mean±SE (n=3).

pair Asp655 and Glu749 of AtlA could be superimposed on the pair Asp86 and Glu177 of cellosyl (Fig. 4B), in agreement with the sequence alignment of AtlA and cellosyl (Fig. 3). The estimated distance of 8.7 Å between Asp655 and Glu749 in AtlA is compatible with the inverting mechanism expected in Cpl-1 (Hermoso *et al*., 2003). Asp747 of AtlA was predicted as a crucial residue as Asp869 of AtlA (*S. mutans*) and Asp771 of AtlH are responsible for lytic activity (Yoshimura *et al*., 2006; Tamura *et al*., 2009); therefore, Asp655, Asp747 and Glu749 in AtlA were assessed as candidates for catalytic active residues. Furthermore, Trp831 and Asp849 of AtlA were conserved residues among lytic enzymes (Fig. 3) and were spatially positioned around the predicted catalytic cavity of AtlA as Trp259 and Asp275 of cellosyl (Fig. 4B).

### Lytic activity of AtlA derivatives

To clarify whether the amino acid residues around the predicted catalytic cavity affect the lytic activity of AtlA, we examined four AtlA mutants, in which one residue was replaced with alanine, constructed by site-directed mutagenesis. Proteins (10 μg) were separated by SDS-PAGE (Fig. 5A). Zymogram analysis of $NaN_3$-treated cells showed that no bands were observed from D655A and D747A and weak bands were found from W831A and D849A (Fig. 5B). The translucent bands were analyzed by ImageJ (Abràmoff *et al*., 2004) and the relative lytic activities of W831A and D849A to wild-type AtlA were 0.05 and 0.23, respectively. Similar results were obtained in the three independent experiments: no lytic activity was observed in D655A and D747A, and a decreased activity was observed in W831A and D849A (Fig. 5C).

## Discussion

The autolysin gene, *atlA*, and its flanking region were first determined in *S. criceti* E49. Sequence analysis indicated the similarity of the adjacent region of *atlA* to that of *atlG* in *S. sobrinus* 6715DP rather than that of *atlA* in *S. mutans* UA159. In *S. sobrinus* 6715DP, a 860-bp intergenic region between *orf1* and *atlG* is observed (Yamada *et al*., 2009), whereas in *S. criceti* E49, a 326-bp intergenic region between *orf5* and *atlA* was found, suggesting that the expression of *atlA* might be different from that of *atlG*. In *S. mutans* UA159, the gene SMU.688, also designated *smu0629*, located 249 bp upstream of the start codon of *atlA,* is required for efficient expression and processing of AtlA (Ahn and Burne, 2007); however, no gene homologous to SMU.688 was observed in the corresponding regions in *S. criceti* and *S. sobrinus*. It is notable that *orf7,* situated in the region just downstream of *atlA* in *S. criceti*, was a homolog of SMU.692 (*thmA*) located in the region downstream of *atlA* in *S. mutans*. The gene products of *thmA* are also required for efficient processing of AtlA in *S. mutans* (Ahn and Burne, 2006), suggesting that the processing of AtlA in *S. criceti* might be associated with the gene products of *orf7*.

The deduced amino acid sequence analysis indicated that AtlA of *S. criceti* was the smallest autolysin in the members of mutans streptococci and predicted AtlA to be a secreted modular enzyme harboring the putative cell-wall-binding domain in the middle and the catalytic domain in the C-terminus. The four 15-residue repeats in the putative cell-wall-binding domain of AtlA are consistent with AtlG and AtlH, compared to five times in AtlA of *S. mutans*. This modular arrangement of AtlA is completely conserved in AtlA of *S. mutans*, AtlG, and AtlH (Shibata *et al*., 2005; Tamura *et al*., 2009; Yamada *et al*., 2009). In contrast, the 1,160-amino-acid autolysin AtlS of *Streptococcus gordonii*, an oral commensal, possesses the *N*-acetylmuramidase domain in the N-terminus (Liu and Burne, 2011), suggesting that various arrangements of modules are preserved in the autolysins of streptococci. Similar findings have been reported in other members of GH25 family that the mature form of LytC of *S. pneumoniae* comprises a choline-binding domain in the N-terminus and a catalytic domain in the C-terminus. Conversely, Cpl-1 of pneumococcal phage Cp-1 carries a catalytic domain in the N-terminus and a choline-binding domain in the C-terminus (Hermoso *et al*., 2003; Pérez-Dorado *et al*., 2010).

The recombinant AtlA with a histidine tag at the C-terminus could be purified in *E. coli* without marked proteolytic cleavage of AtlA. In the zymogram of HF-treated *S. criceti* cells, one 103-kDa band of the recombinant AtlA was observed, whereas two 105- and 72-kDa bands of the SDS extracts of *S. criceti* cells were found. These findings indicate that the recombinant AtlA and SDS extracts of *S. criceti* cells could lyse HF-treated cells. The discrepancy of the 105-kDa band in SDS extracts of *S. criceti* cells with the 103-kDa band of the recombinant AtlA was considered to be due to the processing of AtlA (residues 32–855) to AtlA (residues 65–855), because the construct designed to carry AtlA (residues 32–855) was predicted to be processed by a signal sequence in *E. coli* and be carrying AtlA (residues 65–855). Of note is the fact that the recombinant AtlA showed a weak lytic activity compared to the strong activity of the SDS extracts of *S. criceti*. One possible explanation is that the conformation of the recombinant AtlA constructed in *E. coli* differed from the form of AtlA in SDS extracts of *S. criceti*, and another is that the histidine tag at the C-terminus of the recombinant AtlA might affect its lytic activity.

Zymogram analysis demonstrated that AtlA could lyse cells without HF treatment. It is speculated that AtlA would act as an autolysin for *S. criceti* and play a role in cell separation, as does AtlA of *S. mutans* (Shibata *et al*., 2005). AtlA of *S. mutans* is preserved in two isoforms, 107 and 79 kDa proteins, in SDS extracts (Shibata *et al*., 2005). In the SDS extracts of *S. criceti*, 105- and 72-kDa bands were observed, suggesting that the two proteins might be produced as isoforms of AtlA, presumably in consequence of proteolysis. Further studies such as Western blot analysis using anti-AtlA antibody are needed to verify this hypothesis in AtlA of *S. criceti*.

In the structural characterized GH25 members, the catalytic residues Asp10 and Glu94 of Cpl-1 appear to act as the general base and acid donor in the inverting mechanism, respectively (Hermoso *et al*., 2003). Similarly, in LytC of *S. pneumoniae*, the two acidic residues Asp273 and Glu365 of the mature form (Asp306 and Glu398 of precursor in Fig. 3) are required for a general acid-base mechanism and the

LytC mutant E365Q is inactive (Pérez-Dorado *et al*., 2010); however, it is argued that *Ba*GH25c also acts with net retention of the anomeric configuration (Martinez-Fleites *et al*., 2009). As there was low percentage identity (28% identity) of the catalytic domain of AtlA to the corresponding cellosyl, the model quality assessment became uncertain, as it was pointed that model accuracy steadily increases with increasing sequence identity (Bordoli *et al*., 2009). Indeed, the proposed model of the catalytic domain of AtlA was different from the structure of cellosyl; however, the spatial dispositions of five amino acid residues, Asp655, Asp747, Glu749, Trp831, and Asp849, in the putative catalytic cavity of AtlA resembled those of cellosyl. The Asp86, Asp175, Glu177, and Asp275 of cellosyl are thought to be part of the peptidoglycan-binding sites and contribute to glycan stabilization (Pérez-Dorado *et al*., 2010). It is presumed that Asp655, Asp747, Glu749, and Asp849 of AtlA might be part of the peptidoglycan-binding sites. Trp831 of AtlA was located around the predicted catalytic cavity, suggesting that the aromatic side chain of this residue might be associated with lytic activity. The estimated distance between Asp655 and Glu749 suggested that the catalytic mechanism of AtlA might be an inverting mechanism.

In the process of homology modeling from the template structure, unaligned regions of the target protein by insertion or deletion are predicted as loops (Bordoli *et al*., 2009). Although the accuracy of the homology model is limited, the method has been applied to designing site-directed mutagenesis (Le *et al*., 2004; Chávez-Gutiérrez *et al*., 2006). In our study, zymogram analysis of AtlA mutants demonstrated that Asp655 and Asp747 were critically involved in the lytic activity of AtlA, and Trp831 and Asp849 also affected enzymatic activity. These results were supported by the findings of homology modeling that these residues were thought to be positioned around the catalytic cavity of AtlA.

It is not clear whether calcium ions affect protein structures spatially in GH25 family members. A previous report demonstrated that AtlA of *S. mutans* had no possible motif for calcium binding, although calcium ions enhanced the lytic activity of AtlA (Yoshimura *et al*., 2006). There were no calcium binding motifs in AtlA of *S. criceti*, as in the Dx[DN]xDG motif (Rigden *et al*., 2011). Experimental structure analyses of AtlA would elucidate the predicted catalytic mechanism of Asp655 and Glu749 and the effect of calcium ions on protein structure and lead to development of a drug specific for lysis of cariogenic pathogens.

In conclusion, we first identified the *atlA* gene encoding autolysin AtlA in *S. criceti* and constructed the computational structure of the catalytic domain of AtlA. Residues Asp655 and Asp747 were critical and Trp831 and Asp849 were also related with the lytic activity of AtlA.

## Acknowledgements

This work was supported, in part, by Grants-in-Aid for Scientific Research (23592746), the High-Tech Research Project (2005–2009), Open Research Project (2007–2011), and Strategic Medical Research Center of the Ministry of Education, Culture, Sports, Science, and Technology of Japan.

This work is dedicated to the people facing the earthquake, tsunami, and accidents at Fukushima nuclear power plants in Japan that occurred in March 2011.

## References

**Abràmoff, M.D., Magalhães, P.J., and Ram, S.J.** 2004. Image processing with ImageJ. *Biophotonics International* **11**, 36–42.

**Ahn, S.J. and Burne, R.A.** 2006. The *atlA* operon of *Streptococcus mutans*: role in autolysin maturation and cell surface biogenesis. *J. Bacteriol.* **188**, 6877–6888.

**Ahn, S.J. and Burne, R.A.** 2007. Effects of oxygen on biofilm formation and the AtlA autolysin of *Streptococcus mutans*. *J. Bacteriol.* **189**, 6293–6302.

**Ajdić, D., McShan, W.M., McLaughlin, R.E., Savić, G., Chang, J., Carson, M.B., Primeaux, C., Tian, R., Kenton, S., Jia, H., and *et al.*** 2002. Genome sequence of *Streptococcus mutans* UA159, a cariogenic dental pathogen. *Proc. Natl. Acad. Sci. USA* **99**, 14434–14439.

**Bates, P.A., Kelley, L.A., MacCallum, R.M., and Sternberg, M.J.E.** 2001. Enhancement of protein modeling by human intervention in applying the automatic programs 3D-JIGSAW and 3D-PSSM. *Proteins* **Suppl 5**, 39–46.

**Bordoli, L., Kiefer, F., Arnold, K., Benkert, P., Battey, J., and Schwede, T.** 2009. Protein structure homology modeling using SWISS-MODEL workspace. *Nat. Protoc.* **4**, 1–13.

**Cantarel, B.L., Coutinho, P.M., Rancurel, C., Bernard, T., Lombard, V., and Henrissat, B.** 2009. The Carbohydrate-Active EnZymes database (CAZy): an expert resource for glycogenomics. *Nucleic Acids Res.* **37**, D233–D238.

**Chávez-Gutiérrez, L., Matta-Camacho, E., Osuna, J., Horjales, E., Joseph-Bravo, P., Maigret, B., and Charli, J.L.** 2006. Homology modeling and site-directed mutagenesis of pyroglutamyl peptidase II. Insights into omega-versus aminopeptidase specificity in the M1 family. *J. Biol. Chem.* **281**, 18581–18590.

**Guex, N. and Peitsch, M.C.** 1997. SWISS-MODEL and the Swiss-Pdb Viewer: an environment for comparative protein modeling. *Electrophoresis* **18**, 2714–2723.

**Hamada, S. and Slade, H.D.** 1980. Biology, immunology, and cariogenicity of *Streptococcus mutans*. *Microbiol. Rev.* **44**, 331–384.

**Hanahan, D.** 1983. Studies on transformation of *Escherichia coli* with plasmids. *J. Mol. Biol.* **166**, 557–580.

**Hermoso, J.A., Monterroso, B., Albert, A., Galán, B., Ahrazem, O., García, P., Martínez-Ripoll, M., García, J.L., and Menéndez, M.** 2003. Structural basis for selective recognition of pneumococcal cell wall by modular endolysin from phage Cp-1. *Structure* **11**, 1239–1249.

**Ho, S.N., Hunt, H.D., Horton, R.M., Pullen, J.K., and Pease, L.R.** 1989. Site-directed mutagenesis by overlap extension using the polymerase chain reaction. *Gene* **77**, 51–59.

**Lüthy, R., Bowie, J.U., and Eisenberg, D.** 1992. Assessment of protein models with three-dimensional profiles. *Nature* **356**, 83–85.

**Larkin, M.A., Blackshields, G., Brown, N.P., Chenna, R., McGettigan, P.A., McWilliam, H., Valentin, F., Wallace, I.M., Wilm, A., Lopez, R., and *et al.*** 2007. Clustal W and Clustal X version 2.0. *Bioinformatics* **23**, 2947–2948.

**Laskowski, R.A., MacArthur, M.W., Moss, D.S., and Thornton, J.M.** 1993. PROCHECK: a program to check the stereochemical quality of protein structures. *J. Appl. Cryst.* **26**, 283–291.

**Le, D.T., Yoon, M.Y., Kim, Y.T., and Choi, J.D.** 2004. Homology modeling of the structure of tobacco acetohydroxy acid synthase and examination of the active site by site-directed mutagenesis. *Biochem. Biophys. Res. Commun.* **317**, 930–938.

**Liu, Y. and Burne, R.A.** 2011. The major autolysin of *Streptococcus gordonii* is subject to complex regulation and modulates stress

tolerance, biofilm formation, and extracellular-DNA release. *J. Bacteriol.* **193**, 2826–2837.

**Loesche, W.J.** 1986. Role of *Streptococcus mutans* in human dental decay. *Microbiol. Rev.* **50**, 353–380.

**Martinez-Fleites, C., Korczynska, J.E., Davies, G.J., Cope, M.J., Turkenburg, J.P., and Taylor, E.J.** 2009. The crystal structure of a family GH25 lysozyme from *Bacillus anthracis* implies a neighboring-group catalytic mechanism with retention of anomeric configuration. *Carbohydr. Res.* **344**, 1753–1757.

**Page, R.D.M.** 1996. TreeView: an application to display phylogenetic trees on personal computers. *Comput. Appl. Biosci.* **12**, 357–358.

**Pérez-Dorado, I., González, A., Morales, M., Sanles, R., Striker, W., Vollmer, W., Mobashery, S., García, J.L., Martínez-Ripoll, M., García, P., and *et al.*** 2010. Insights into pneumococcal fratricide from the crystal structures of the modular killing factor LytC. *Nat. Struct. Mol. Biol.* **17**, 576–581.

**Pettersen, E.F., Goddard, T.D., Huang, C.C., Couch, G.S., Greenblatt, D.M., Meng, E.C., and Ferrin, T.E.** 2004. UCSF Chimera–a visualization system for exploratory research and analysis. *J. Comput. Chem.* **25**, 1605–1612.

**Rau, A., Hogg, T., Marquardt, R., and Hilgenfeld, R.** 2001. A new lysozyme fold. Crystal structure of the muramidase from *Streptomyces coelicolor* at 1.65 Å resolution. *J. Biol. Chem.* **276**, 31994–31999.

**Rigden, D.J., Woodhead, D.D., Wong, P.W.H., and Galperin, M.Y.** 2011. New structural and functional contexts of the Dx[DN]xDG linear motif: insights into evolution of calcium-binding proteins. *PLoS ONE* **6**, e21507.

**Shibata, Y., Kawada, M., Nakano, Y., Toyoshima, K., and Yamashita, Y.** 2005. Identification and characterization of an autolysin-encoding gene of *Streptococcus mutans*. *Infect. Immun.* **73**, 3512–3520.

**Tamura, H., Yamada, A., and Kato, H.** 2007. Identification and characterization of a dextranase gene of *Streptococcus criceti*. *Microbiol. Immunol.* **51**, 721–732.

**Tamura, H., Yamada, A., Yoshida, Y., and Kato, H.** 2009. Identification and characterization of an autolysin gene, *atlh*, from *Streptococcus downei*. *Curr. Microbiol.* **58**, 432–437.

**Yamada, A., Tamura, H., and Kato, H.** 2009. Identification and characterization of an autolysin gene, *atlg*, from *Streptococcus sobrinus*. *FEMS Microbiol. Lett.* **291**, 17–23.

**Yoshimura, G., Komatsuzawa, H., Hayashi, I., Fujiwara, T., Yamada, S., Nakano, Y., Tomita, Y., Kozai, K., and Sugai, M.** 2006. Identification and molecular characterization of an *N*-acetylmuraminidase, Aml, involved in *Streptococcus mutans* cell separation. *Microbiol. Immunol.* **50**, 729–742.